G protein-coupled estrogen receptor activation by Bisphenol-A disrupts protection from apoptosis conferred by estrogen receptors ERα and ERβ in pancreatic beta cells

Ignacio Babiloni-Chust[1,2,*], Reinaldo S. dos Santos[1,2,*], Regla M. Medina-Gali[1,2], Atenea A. Perez-Serna[1,2], José-Antonio Encinar[1], Juan Martinez-Pinna[3,1], Jan-Ake Gustafsson[4,5], Laura Marroqui[1,2] and Angel Nadal[1,2]

1. Instituto de Investigación, Desarrollo e Innovación en Biotecnología Sanitaria de Elche (IDiBE), Universidad Miguel Hernández de Elche, Elche, Spain.
2. Centro de Investigación Biomédica en Red de Diabetes y Enfermedades Metabólicas Asociadas (CIBERDEM), Spain. www.ciberdem.org
3. Departamento de Fisiología, Genética y Microbiología, Universidad de Alicante, Alicante, Spain.
4. Department of Cell Biology and Biochemistry, Center for Nuclear Receptors and Cell Signaling, University of Houston, Houston, TX, USA.
5. Department of Biosciences and Nutrition, Karolinska Institutet, Huddinge, Sweden

* Ignacio Babiloni-Chust and Reinaldo S. dos Santos contributed equally to this work.

Corresponding author

Angel Nadal, Instituto de Investigación, Desarrollo e Innovación en Biotecnología Sanitaria de Elche (IDiBE), Universidad Miguel Hernández de Elche, 03202-Elche, Alicante, Spain.

E-mail: nadal@umh.es

Keywords

Apoptosis, Bisphenol-A, Endocrine disruptors, GPER/GPR30, Heterodimers, 17β-estradiol, Estrogen receptors.

Abbreviations

BERKO: Estrogen Receptor β knockout

BPA: Bisphenol-A

DCF: 2',7'-Dichlorofluorescein diacetate

E2: 17β-estradiol

ER: Estrogen receptor

ERα: Estrogen receptor α

ERβ: Estrogen receptor β

GPER: G protein-coupled estrogen receptor

LBD: Ligand binding domain

MPP: Methylpiperidinopyrazole

PHTPP: 4-(2-phenyl-5,7-bis(trifluoromethyl)pyrazolo[1,5-a]pyrimidin-3-yl)phenol

PLA: Proximity ligand assay

ROS: Reactive oxygen species

siRNA: Small interfering RNA

Abstract

17β-estradiol protects pancreatic β-cells from apoptosis via the estrogen receptors ERα, ERβ and GPER. Conversely, the endocrine disruptor Bisphenol-A (BPA), which exerts multiple effects in this cell type via the same estrogen receptors, increased basal apoptosis. The molecular initiated events that trigger these opposite actions have yet to be identified. We demonstrated that combined genetic downregulation and pharmacological blockade of each estrogen receptor increased apoptosis to a different extent. The increase in apoptosis induced by BPA was diminished by the pharmacological blockade or the genetic silencing of GPER, and it was partially reproduced by the GPER agonist G1. BPA and G1-induced apoptosis were abolished upon pharmacological inhibition, silencing of ERα and ERβ, or in dispersed islet cells from ERβ knockout (BERKO) mice. Yet, the ERα and ERβ agonists, PPT and DPN, respectively, had no effect on beta cell viability. To exert their biological actions, ERα and ERβ form homodimers and heterodimers. Molecular dynamic simulations together with proximity ligand assay and coimmunoprecipitation experiments indicated that the interaction of BPA with ERα and ERβ as well as the GPER activation by G1 decreased ERαβ heterodimers. We propose that ERαβ heterodimers play an antiapoptotic role in beta cells and that BPA- and G1-induced decrease in ERαβ heterodimers leads to beta cell apoptosis. Unveiling how different estrogenic chemicals affect the crosstalk among estrogen receptors should help to identify diabetogenic endocrine disruptors.

Highlights

- Pharmacological blockade and gene silencing of estrogen receptors ERα, ERβ and GPER indicate that they are antiapoptotic in basal conditions.
- GPER activation by G1 and BPA triggered apoptosis via a crosstalk with ERα and ERβ.
- BPA interaction with ERα and ERβ as well as GPER activation decreased ERαβ heterodimers, which was associated to increased apoptosis.
- This pathway represents a novel molecular initiating event underlying the pro-apoptotic effect of BPA
- The EndoC-βH1 cell line may be a valid model of human β-cells for identifying diabetogenic pollutants.

1. Introduction

Loss of functional beta cell mass is a critical component contributing to the hyperglycemia observed in individuals with type 1 or type 2 diabetes. The interaction between the individual genetic background and environmental factors determines the progression of beta cell dysfunction and death (Eizirik et al., 2020).

Sex differences exist in the prevalence of diabetes. Premenopausal women have a lower incidence of diabetes compared with men (Gannon et al., 2018; Kautzky-Willer et al., 2016). These sex differences can be partially attributed to the actions of 17β-estradiol (E2) through three estrogen receptors (ERs), namely estrogen receptors α (ERα) and β (ERβ) (Heldring et al., 2007) and the G protein-coupled estrogen receptor (GPER/GPR30) (Revankar et al., 2005; Thomas et al., 2005). After ligand binding, ERα and ERβ can either form homo- and heterodimers and act as transcription factors or tether other DNA-bound transcription factors (Heldring et al., 2007). In addition to their nuclear-initiated actions, ERα and ERβ can trigger extranuclear-initiated effects after dimerization and activate a variety of signaling pathways (Levin and Hammes, 2016).

All three ERs protect beta cells from different apoptotic insults (Balhuizen et al., 2010; le May et al., 2006; Liu et al., 2009), yet the role of E2 can be disrupted by environmental chemicals that compete for the same receptors and modify the physiological pathways activated by the natural hormone (Gore et al., 2015). Bisphenol-A (BPA), which is used as a model of endocrine disrupting chemical that alters insulin secretion and insulin sensitivity in mice (Alonso-Magdalena et al., 2010, 2006), has been implicated in the etiology of diabetes (Alonso-Magdalena et al., 2011; Sargis and Simmons, 2019). At concentrations similar to those found in human blood (Vandenberg et al., 2010), BPA increases pancreatic insulin content via ERα (Alonso-Magdalena et al., 2008) and regulates ion channel expression and function as well as augments insulin release in an ERβ-mediated manner (Marroqui et al., 2021; Martinez-Pinna et al., 2019; Soriano et al., 2012). In INS-1 cells and mouse dispersed islet cells, BPA induces mitochondrial dysfunction, ROS production and NF-κB activation, which culminates in beta cell apoptosis (Carchia et al., 2015; Lin et al., 2013).

As E2 and BPA have opposite actions on beta cell survival, we decided to investigate the molecular initiating event (MIE) (Allen et al., 2014) underlying the pro-apoptotic effect of BPA.

Using several beta cell models, including the EndoC-βH1 cell line, which is a valid model of human beta cells recommended for screening studies (Tsonkova et al., 2018), we show

113 that ERα, ERβ and GPER mediate beta cell survival. Our findings suggest that ERαβ
114 heterodimerization is key to this antiapoptotic role and that G1, a GPER agonist, and BPA
115 induce apoptosis via a mechanism involving the reduction in ERαβ heterodimers
116 downstream of GPER.
117
118 **2. Material and methods**
119
120 **2.1. Chemical substances and animals**
121 Bisphenol-A was purchased from MP Biomedicals (Cat no. 155118; Santa Ana, CA,
122 USA). 17β-estradiol (E2, Cat no. E8875) was obtained from Sigma-Aldrich (Saint Louis,
123 MO, USA). Propylpyrazoletriol (PPT, Cat no. 1426), Diarylpropionitrile (DPN, Cat no.
124 1494), G1 (Cat no. 3577), ICI 182,780 (Cat no. 1047), PHTPP (Cat no. 2662) and
125 Methylpiperidinopyrazole (MPP, Cat no. 1991) were obtained from Tocris Cookson
126 (Bristol, UK).
127 Mice with knockout of the *Erβ* gene (also known as *Esr2*) (BERKO mice), supplied by
128 Jan-Åke Gustafsson's laboratory, were generated as described (Krege et al., 1998). Wild-
129 type littermates and BERKO mice were obtained from the same supplier and colony and
130 kept under standard housing conditions (12 h light/dark cycle, food *ad libitum*).
131 Experimental procedures were performed according to the Spanish Royal Decree
132 1201/2005 and the European Community Council directive 2010/63/EU. The ethical
133 committee of Miguel Hernandez University reviewed and approved the methods used
134 herein (approvals ID: UMH-IB-AN-01–14 and UMH-IB-AN-02-14).
135
136 **2.2. Culture of cell lines and dispersed islet cells**
137 Rat insulin-producing INS-1E cells (RRID: CVCL_0351, kindly provided by Dr. C.
138 Wollheim, Department of Cell Physiology and Metabolism, University of Geneva,
139 Geneva, Switzerland) were cultured as previously described (Santin et al., 2016). Human
140 insulin-producing EndoC-βH1 cells (RRID: CVCL_L909, Univercell-Biosolutions,
141 France) were cultured in Matrigel/fibronectin-coated plates as described before
142 (Ravassard et al., 2011). INS-1E and EndoC-βH1 cells have been shown to be free of
143 mycoplasma infection. Pancreatic islets were isolated using collagenase (Sigma, St Louis,
144 MO, USA) as described (Alonso-Magdalena et al., 2008). Islets were dispersed into single
145 cells and cultured in polylysine-coated plates as described before (Martinez-Pinna et al.,

146 2019). Cell lines and dispersed cells were kept at 37°C in a humidified atmosphere of
147 95% O_2 and 5% CO_2.
148
149 **2.3. RNA interference**
150 Optimal siRNA concentration (30 nM) and conditions for small interfering RNA (siRNA)
151 transfection using Lipofectamine RNAiMAX lipid reagent (Invitrogen, Carlsbad, CA,
152 USA) were previously established (Santin et al., 2016). Allstars Negative Control siRNA
153 (Qiagen, Venlo, the Netherlands) was used as a negative control (siCTRL). siRNA
154 targeting *Erα* (also known as *Esr1*; si*ERα*), *Erβ* (si*ERβ*) or *Gper1* (si*GPER1*) (Qiagen,
155 Venlo, the Netherlands) were used herein (Supplementary Table 2). Of note, GPER
156 silencing in INS-1E cells as well as ERα and ERβ silencing in EndoC-βH1 cells were
157 performed in a two-step transfection protocol (Marroqui et al., 2015). Briefly, cells were
158 exposed to 30 nmol/l siCTRL or si*GPER1*/si*Gper1* for 16 h, washed and allowed to
159 recover in culture for 24 h. Next, cells were exposed again to the same siRNAs for 16 h,
160 allowed to recover in culture for 48 h, and then used for the subsequent experiments.
161 Transfections with siRNAs were carried out in BSA- and antibiotic-free medium.
162
163 **2.4. Cell viability assessment by DNA-binding dyes**
164 Percentage of apoptosis was determined after staining with the DNA-binding dyes
165 Hoechst 33342 and propidium iodide as described (Santin et al., 2016). To avoid bias,
166 cell viability was assessed by two different observers, being one of them unaware of
167 sample identity. The agreement of results between both observes was higher than 90%.
168
169 **2.5. Flow cytometric analysis**
170 Apoptotic cells were analyzed by flow cytometry using the FITC Annexin V Apoptosis
171 Detection Kit with propidium iodide (BioLegend, San Diego, CA, USA) following the
172 manufacturer's instructions. Briefly, INS-1E cells were detached and dissociated using
173 Accutase (Thermo Fisher Scientific). Cell suspension was washed twice with PBS (200
174 *g* for 7 min) and proceeded to Annexin V-fluorescein isothiocyanate (FITC)/PI staining
175 according to the manufacturer's instructions (FITC Annexin V Apoptosis Detection Kit
176 with PI; BioLegend, San Diego, CA, USA). Cells stained with Annexin V (both Annexin
177 V^+- and Annexin V^+/PI^+-cells) were detected using a FACSCanto II (BD Biosciences,
178 Madrid, Spain) flow cytometer.
179

180

181 **2.6. Caspase 3/7 activity**

182 Caspase 3/7 activity was determined using the Caspase-Glo® 3/7 assay (Promega,
183 Madison, WI, USA) following the manufacturer's instructions. Briefly, following
184 treatment, cells were incubated with Caspase-Glo® 3/7 reagent at room temperature
185 before recording luminescence with a POLASTAR plate reader (BMG Labtech,
186 Germany).

187

188 **2.7. MTT assay**

189 Cell viability was measured by the colorimetric assay showing reduction of MTT (3-(4,5-
190 dimethylthiazol-2-yl)-2,5-diphenyltetrazolium bromide) (Sigma-Aldrich) as previously
191 described (Denizot and Lang, 1986; Mosmann, 1983). Briefly, MTT prepared in RPMI
192 1640 without phenol red was added (final concentration: 0.5 mg/ml) and incubated at
193 37°C for 3 h. Upon incubation, the supernatant was aspirated and 100 ml DMSO was
194 added to dissolve formazan crystals. The absorbance was measured at 595 nm using an
195 iMark™ Microplate absorbance reader (Bio-Rad, Hercules, CA) and the percentage of
196 cell viability was calculated.

197

198 **2.8. Real-time PCR**

199 Quantitative RT-PCR was carried out in a CFX96 Real-Time System (Bio-Rad
200 Laboratories, Hercules, CA, USA). RNA was extracted with the RNeasy Micro kit
201 (Qiagen) and cDNA prepared with the High-Capacity cDNA Reverse Transcription kit
202 (Applied Biosystems, Foster City, CA, USA). Amplification reactions were performed as
203 describe (Villar-Pazos et al., 2017). Values were analyzed with CFX Manager Version
204 1.6 (Bio-Rad) and expressed as the relative expression in respect of control values ($2^{-\Delta\Delta Ct}$)
205 (Schmittgen and Livak, 2008). *Gapdh* and β-actin were used as housekeeping genes for
206 rat and human samples, respectively. The primers used herein are listed in Supplementary
207 Table 2.

208

209 **2.9. DCF assay**

210 Oxidative stress was measured using the fluorescent probe 2',7'-dichlorofluorescein
211 diacetate (DCF; Sigma-Aldrich) as described (Cunha et al., 2016). Briefly, cells seeded
212 in 96-well black plates were loaded with 10 μM DCF for 30 min at 37°C and washed with

213 PBS. DCF fluorescence was quantified in a POLASTAR plate reader (BMG Labtech,
214 Germany). Data are expressed as DCF fluorescence corrected by total protein.
215
216 **2.10. Western blotting**
217 Cells were washed with cold PBS and lysed in Laemmli buffer. Immunoblot analysis was
218 performed by overnight incubation with the antibodies against ERα, ERβ, GPER, β-actin,
219 GAPDH and α-tubulin. Afterwards, membranes were incubated for 1 h at room
220 temperature with peroxidase-conjugated antibodies (1:5000) as secondary antibodies.
221 SuperSignal West Femto chemiluminescent substrate (Thermo Scientific, Rockford, IL,
222 USA) and ChemiDoc XRS+ (Bio-Rad Laboratories) were used to detect immunoreactive
223 bands. Densitometry analysis was done with the Image Lab software (version 4.1, Bio-
224 Rad Laboratories). The antibodies used herein are listed in Supplementary Table 3.
225
226 **2.11. In situ proximity ligation assay (PLA)**
227 In situ PLA was performed using a Duolink® In Situ Red Starter Kit (Sigma-Aldrich)
228 following the manufacturer's instructions with slight modifications (INCLUDE Iwabuchi
229 E, Miki Y, Ono K, et al, J Steroid Biochem Mol Biol 165:159–169, 2017)(Iwabuchi et
230 al., 2017). Briefly, cells grown on coverslips were washed with PBS and fixed with 4%
231 paraformaldehyde (VWR Chemicals, Spain). Then, cells were washed with PBS and
232 permeabilized with 0.1% Triton-X-100. Subsequently, cells were incubated for 30 min at
233 37ºC with a blocking solution and incubated overnight at 4ºC with the corresponding
234 primary antibodies (Supplementary Table 3). PLA probe solution was added and
235 incubated for 1 h at 37ºC. Ligation-Ligase solution was added, and coverslips were
236 incubated for 30 min at 37ºC. Subsequently, amplification-polymerase solution was
237 added and incubated for 100 min at 37ºC. Of note, all incubations at 37ºC were carried
238 out using a pre-heated humidity chamber. Finally, coverslips were washed with a specific
239 buffer provided and mounted with a minimal volume of Duolink in situ Mounting
240 Medium with DAPI®. ER dimers were observed using a Zeiss Confocal LSM900
241 microscope equipped with a camera (Zeiss-Vision, Munich, Germany) and images were
242 acquired at x63 magnification and analyzed using ZEN software (version 3.2; Zeiss-
243 Vision, Munich, Germany).
244
245 **2.12. Co-immunoprecipitation**

246 INS-1E cells were washed with cold PBS, lysed in cold immunoprecipitation buffer (50
247 mmol/l Tris, pH 7.5, 4 mmol/l NaCl, 2 mmol/l $MgCl_2$, 10 mmol/l NaF, 1 mmol/l PMSF,
248 1% Triton X-100 and Complete Protease inhibitor mixture, Roche Diagnostics) for 30
249 min on ice and centrifuged at 20,000 *g* for 10 min at 4ºC. Cell lysates were pre-cleared
250 for 1 h at 4ºC with Dynabeads Protein G (Thermo Fischer Scientific; Cat no. 10003D).
251 The same amounts of protein were incubated overnight at 4ºC, either with an anti-ERβ
252 antibody or nonspecific rabbit IgG (Santa Cruz Biotechnology) used as negative control.
253 Upon overnight incubation, Immunoprecipitates were incubated for 1 h at 4ºC with
254 Dynabeads Protein G, washed six times with cold immunoprecipitation buffer and
255 resuspended in 5x Laemmli buffer. Immunoprecipitates and total protein (Input) were
256 subjected to SDS-PAGE and immunoblotted with mouse anti-ERα antibody. The
257 antibodies used herein are listed in Supplementary Table 3.
258
259 **2.13. Molecular docking and dynamics simulations**
260 More than 300 human ERα-ligand-binding domain (LBD) (UniProt code: P03372) and
261 32 human ERβ-LBD (UniProt code: Q92731) structures were resolved from
262 cryptographic data. As these structures contained unresolved residues in mobile regions
263 of the protein that diffracted poorly, the lost amino acids were reconstructed after
264 generation of a homology model at the Swiss-Model server (Biasini et al., 2014; Marroqui
265 et al., 2021). After unresolved gaps elimination, models for the hERα-LBD monomer
266 (Protein Data Bank entry 5DXE as template) and the hERβ-LBD monomer (Protein Data
267 Bank entry 3OLS as template) were generated. From these monomeric structures homo-
268 and heterodimers were reconstructed using GRAMM-X server (Tovchigrechko and
269 Vakser, 2006). E2 and BPA molecular docking simulations within the cavity of each LBD
270 were performed using the YASARA structure software (version 20.12.24) (Marroqui et
271 al., 2021). Molecular dynamics simulations on the structures with the best docking
272 calculations were performed with YASARA structure software (version 20.10.24)
273 (Marroqui et al., 2021). The intermolecular protein interaction energy for homo- and
274 heterodimers subunits was calculated using the Folds 5.0 software (Delgado et al., 2019).
275
276 **2.14. Statistical analysis**
277 Experimenters were not blind to group assignment and outcome assessment. GraphPad
278 Prism 7.0 software (GraphPad Software, La Jolla, CA, USA; www.graphpad.com) was
279 used for all statistical analyses. Data are expressed as the mean ± SEM. To assess

differences between groups, we used two-tailed Student's *t* test or ANOVA when appropriate. For nonparametric data we used Mann–Whitney and Kruskal–Wallis ANOVA tests (followed by Dunn's test), depending on the experimental groups involved in the comparison. A p value ≤ 0.05 was considered statistically significant.

284 **3. Results**

285 In INS-1E (Fig. 1a) and EndoC-βH1 cells (Fig. 1b), E2 (10 pM/l to 1 μM) either had no
286 effect or decreased apoptosis. Conversely, BPA increased apoptosis in both cell lines in
287 a dose-dependent manner (Fig. 1c,d). Similar results were observed in dispersed islet cells
288 from female mice (Fig. 1e). These results were confirmed by three other approaches,
289 namely flow cytometry analysis (Fig. 1f), caspase 3/7 activity (Fig. 1g) and MTT assay
290 (Supplementary Fig. 1). When E2 and BPA were added together, E2 1 nM prevented
291 BPA-induced apoptosis (Fig. 1h), suggesting that E2 and BPA initiate common pathways.
292 Previous work demonstrated that BPA induces oxidative stress in beta cells (Carchia et
293 al., 2015; Lin et al., 2013). Similarly, we observed that BPA upregulated genes encoding
294 the antioxidant enzymes, superoxide dismutase (*Sod2*), glutathione peroxidase 4 (*Gpx4*)
295 and catalase (*Cat*) (Supplementary Fig. 2a-c) and increased reactive oxygen species
296 (ROS) generation (Supplementary Fig. 2d,e). The antioxidant N-acetylcysteine abolished
297 BPA-induced ROS production in INS-1E (Supplementary Fig. 2d) and EndoC-βH1 cells
298 (Supplementary Fig. 2e). Notably, N-acetylcysteine prevented BPA-induced apoptosis in
299 both cell lines (Supplementary Fig. 2f,g), reinforcing that oxidative stress is involved in
300 BPA-induced apoptosis. Of note, E2 did not change ROS levels (data not shown). These
301 results indicate that ROS production is a key event involved in BPA-induced beta cell
302 apoptosis.

303 As previous results indicate that BPA acts via ERs in beta cells (Alonso-Magdalena et al.,
304 2008; Martinez-Pinna et al., 2019; Soriano et al., 2012) we evaluated the expression of
305 ERα, ERβ and GPER in INS-1E and EndoC-βH1 cells by quantitative RT-PCR and
306 western blot. Considering ERα expression as 1, mRNA analyses showed that the ratio
307 GPER:ERα:ERβ was 100:1:0.3 for INS-1E (Supplementary Fig. 3a) and 675:1:3.3 for
308 EndoC-βH1 cells (Supplementary Fig. 3b). This expression pattern was confirmed at
309 protein level, where GPER was the most expressed of the three receptors (Supplementary
310 Fig. 3c).

311

312 **3.1. GPER mediates BPA-induced apoptosis**

313 We first assessed whether GPER participated in BPA-induced apoptosis. GPER
314 antagonist G15 reduced BPA-triggered apoptosis in INS-1E and EndoC-βH1 cells (Fig.
315 2a,b). Doses as low as 100 pM of the GPER agonist G1 induced apoptosis in INS-1E cells
316 (Supplementary Fig. 4a). In comparison with BPA 1 nM, G1 100 nM presented a
317 significantly smaller effect on apoptosis in both cell lines (Fig. 2c,d). To further study the

318 GPER role in beta cell survival, we used siRNAs to inhibit GPER expression in INS-1E
319 and EndoC-βH1 cells (Fig. 2e-j, Supplementary Fig. 4b,c). GPER silencing promoted
320 apoptosis in basal conditions in INS-1E but not in EndoC-βH1 cells (Fig. 2f,i). Moreover,
321 GPER-inhibited cells were less susceptible to BPA-induced apoptosis than control cells
322 (Fig. 2f,g,i,j). Similar data were obtained with a second, independent siRNA (data not
323 shown). These results indicate that GPER activation is part of the mechanism whereby
324 BPA elicits apoptosis.
325
326 **3.2. ERα and ERβ are involved in BPA-induced apoptosis**
327 We then investigated whether ERα and ERβ were also implicated in BPA-induced
328 apoptosis. In both cell lines, the pure antiestrogen ICI 182,780 abolished the BPA effect
329 on apoptosis (Fig. 3a,b). Treatment with the ERα antagonist methylpiperidinopyrazole
330 (MPP) induced apoptosis in basal conditions, while propylpyrazoletriol (PPT) an ERα
331 agonist, did not change viability (Fig. 3c, Supplementary Fig. 5a,b). In INS-1E cells, MPP
332 abolished BPA-induced apoptosis (Fig. 3c). To further characterize ERα participation in
333 cell survival and BPA-induced apoptosis, we silenced ERα expression in INS-1E and
334 EndoC-βH1 cells using specific siRNAs (Fig. 3d,g, Supplementary Fig. 5c-e). ERα
335 knockdown augmented apoptosis in basal conditions and prevented BPA-induced
336 apoptosis in both cell lines (Fig. 3e,f,h,i). We confirmed these data with a second,
337 independent siRNA (data not shown).
338 Regarding ERβ, while its antagonist 4-(2-phenyl-5,7-bis(trifluoromethyl)pyrazolo[1,5-
339 a]pyrimidin-3-yl)phenol (PHTPP) also induced apoptosis in basal conditions, ERβ
340 agonist diarylpropionitrile (DPN) had no effect on beta cell viability (Fig. 4a,
341 Supplementary Fig. 6a,b). ERβ inhibition by siRNAs (Fig. 4c,f, Supplementary Fig. 6c-
342 h) induced a substantial increase in apoptosis, mainly in INS-1E cells; importantly, BPA-
343 elicited apoptosis was partially lost following ERβ silencing (Fig. 4d,e,g,h). Comparable
344 results were observed with a second, independent siRNA (data not shown). Finally, BPA
345 effects on viability were abrogated in dispersed islets cells from BERKO mice (Fig. 4b).
346
347 **3.3. A crosstalk among ERα, ERβ and GPER mediates beta cell survival**
348 As our data indicate that GPER signaling triggers beta cell apoptosis via downstream
349 activation of ERα and ERβ, we sought to examine this hypothesis. First, we observed that
350 G1-induced apoptosis was abolished by the antiestrogen ICI 182,780 (Fig. 5a,b). As G1
351 may also bind to and activate a 36-kDa variant of ERα, ERα36 (Kang et al., 2010), we

352 silenced GPER (Fig. 5c, Supplementary Fig. 7a) to test whether G1 affected apoptosis via
353 GPER. Notably, G1 did not affect apoptosis in GPER-silenced cells (Fig. 5d,
354 Supplementary Fig. 7b), indicating that, in our cell system, G1 acts preferentially through
355 GPER. Moreover, MPP (ERα antagonist) and PHTPP (ERβ antagonist) prevented G1-
356 induced apoptosis (Fig. 5e-h). We then tested G1 effects on apoptosis upon silencing of
357 ERα or ERβ separately (si*Erα* and si*Erβ*) or simultaneously (si*Erα*/*Erβ*) (Fig. 5i,
358 Supplementary Fig. 7c-e). As described above, ERα or ERβ knockdown induced beta cell
359 death and silencing of both receptors simultaneously induced apoptosis to the same extent
360 observed in ERβ-inhibited cells (Fig. 5i, Supplementary Fig. 7f). G1 effect on apoptosis
361 was lost in ERα-, ERβ- or ERα/ERβ-deficient cells (Fig. 5i, Supplementary Fig. 7f).
362 Lastly, G1 induced apoptosis in dispersed islet cells from WT mice but its effect on
363 apoptosis was completely blunted in dispersed cells from BERKO mice (Fig. 5j). These
364 results indicate that ERβ seems to be more important than ERα for beta cell survival and
365 that ERα and ERβ are required for GPER effects on viability.
366
367 **3.4. ER heterodimerization**
368 After ligand binding, ERα and ERβ form homodimers and heterodimers to exert their
369 biological actions (Levin and Hammes, 2016; Razandi et al., 2004). As our data suggest
370 that part of the BPA effect on apoptosis is directly mediated by ERα and ERβ, we sought
371 to study if the binding of E2 or BPA would stabilize ER homo- and/or heterodimers. We
372 performed docking and molecular dynamics simulations using human structural models
373 of ERα and ERβ. Our models were obtained from resolved dimeric structures of the ER
374 LBD where the protein is co-crystallized with ligands, E2 and BPA, bound to the LBD
375 cavity that is closed by the transactivation helix H12 (Fig. 6a-c). Figure 6 depicts models
376 of the ERα-ERα homodimer (ERαα; Fig. 6a), ERβ-ERβ homodimer (ERββ; Fig. 6b) and
377 ERα-ERβ heterodimer (ERαβ; Fig. 6c).
378 Molecular docking simulations resulted in lower Gibbs free energy changes for E2 (-
379 11.05 and -10.86 kcal/mol for hERα-LBD and hERβ-LBD, respectively) compared with
380 BPA (-8.15 and -8.37 kcal/mol for hERα-LBD and hERβ-LBD, respectively). These
381 values are similar to those observed for rat ERs (Marroqui et al., 2021) and agree with the
382 higher affinity of both receptors for E2 (compared with BPA) (Kuiper et al., 1997). We
383 used these protein-ligand complexes as the starting point to initiate molecular dynamics
384 simulations of the ligands within the cavity during 200 ns. Then, we analyzed the
385 monomer-monomer interaction energy (Fig. 6d-f), the trajectory of the ligands within the

386 LBD pocket (Supplementary Fig. 8) and the solvation binding energy of E2 and BPA
387 bound to the LBD cavity (Fig. 6g-i).
388 When we examined the monomer-monomer interaction energy with E2 or BPA bound to
389 both cavities of the LBD, we found that, for ERαα homodimers, the frequency distribution
390 of the intermolecular interaction energy between monomers was lower for E2 than for
391 BPA (Fig. 6d). This indicates that E2 stabilizes ERαα homodimer more than BPA. For
392 ERββ homodimers, E2 and BPA presented a similar interaction energy, suggesting a
393 comparable ERββ stabilization with both ligands (Fig. 6e). When the interaction energy
394 for ERαβ heterodimers was analyzed, E2 presented a much lower interaction energy than
395 BPA, indicating that BPA does not stabilize heterodimers (Fig. 6f). The trajectory of E2
396 and BPA within the cavity behaves differently; E2 showed minimal deviations during the
397 200 ns simulation time for both homodimers and for the heterodimer (Supplementary Fig.
398 8), suggesting a high stability of the hormone within the LBD pocket in the homo- and
399 heterodimers. Conversely, BPA shows rapid structural rearrangements for both
400 homodimers and heterodimers (Supplementary Fig. 8), a behavior previously showed for
401 monomers (Li et al., 2018; Marroqui et al., 2021). This suggests a less stable binding of
402 BPA compared to E2 for the three configurations of dimers.
403 To investigate the binding affinity of both ligands in homo- and heterodimers we analyzed
404 the frequency distribution of the solvation binding energy values of E2 and BPA bound
405 to each type of dimer (Wang et al., 2016) (Fig. 6g-i). Of note, positive values indicate
406 strong ligand-protein binding (Marroqui et al., 2021). E2 binding to both homodimer
407 cavities, LBD-ERαα (Fig. 6g) and LBD-ERββ (Fig. 6h), shows very similar values. In the
408 heterodimer, however, the solvation energy values were higher for E2 binding to the ERα
409 monomer forming the heterodimer (75 kcal/mol) than for E2 binding to the ERβ monomer
410 of the heterodimer (63 kcal/mol) (Fig. 6i). For BPA, the solvation binding energy values
411 for homodimers were 30-35 kcal/mol for LBD-ERαα (Fig. 6g) and 55-60 kcal/mol for
412 LBD-ERββ (Fig. 6i), which indicates that BPA showed higher affinity for ERββ than for
413 ERαα. When we analyzed the LBD-ERαβ, the frequency distribution of the solvation
414 energy deviates from a Gaussian distribution, especially for BPA bound to the beta
415 subunit of the heterodimer (Fig. 6i). This suggests a much lower BPA affinity for LBD-
416 ERαβ compared with LBD-ERββ. In summary, these simulations indicate that BPA
417 affinity is higher for ERββ than for ERαα and ERαβ. Binding of E2 should stabilize the
418 three forms, preferentially ERαα, while BPA would mainly stabilize ERββ, to a much
419 less extent ERαα and does not stabilize ERαβ.

420 To further explore how E2, BPA and G1 affect heterodimer formation we performed in
421 situ proximity ligand assay (PLA) and co-immunoprecipitation. The PLA analysis
422 showed a small number of heterodimers (shown as red dots) in vehicle-treated cells,
423 which greatly increased upon E2 exposure for 24 h (Fig. 7a, Veh and E2 panels). In the
424 presence of BPA or G1, however, very few red dots were observed, suggesting that these
425 compounds decreased heterodimer formation (Fig. 7a, BPA and G1 panels). Co-
426 immunoprecipitation assay indicated that ERα directly bound to ERβ (Fig. 7b-e). In
427 agreement with the PLA data, the interaction between ERα and ERβ was augmented by
428 E2 and significantly reduced by BPA (Fig. 7b,c) and G1 (Fig. 7d,e). Altogether, these
429 results suggest that E2 promotes ERαβ heterodimerization while BPA and G1 seemed to
430 disrupt ERαβ formation.
431
432 **4. Discussion**
433 BPA is an endocrine disruptor with diabetogenic properties (Alonso-Magdalena et al.,
434 2011; Sargis and Simmons, 2019). In adult mice, BPA increases serum insulin levels and
435 induces insulin resistance (Alonso-Magdalena et al., 2006). When administered to
436 pregnant mice, BPA altered insulin release, beta cell mass and the metabolome in male
437 offspring (Alonso-Magdalena et al., 2010; Bansal et al., 2017; Cabaton et al., 2013) and
438 alters glucose homeostasis in mothers later in life (Alonso-Magdalena et al., 2015, 2010).
439 In humans, BPA rapidly changed plasma insulin levels (Stahlhut et al., 2018) and
440 epidemiological studies have linked BPA exposure to type 2 diabetes development
441 (Rancière et al., 2019; Wang et al., 2019). Here we show that environmentally relevant
442 doses of BPA increase beta cell apoptosis in an ERα-, ERβ- and GPER-dependent
443 manner. Moreover, molecular dynamic simulations together with PLA and co-
444 immunoprecipitation data indicate that BPA binding to ERα and ERβ as well as GPER
445 activation decreased ERαβ heterodimers.
446 It has been shown that E2 protects beta cells from several pro-apoptotic stimuli, such
447 oxidative stress (le May et al., 2006), proinflammatory cytokines (Contreras et al., 2002)
448 and high glucose (Kooptiwut et al., 2018). These studies suggest that ERα is crucial for
449 pancreatic islet survival. For instance, E2 prevented streptozotocin-induced beta cell
450 apoptosis in vivo and protected mice from insulin-deficient diabetes in an ERα-dependent
451 manner (le May et al., 2006). Furthermore, ERα preserved mitochondrial function and
452 attenuated endoplasmic reticulum stress in a context where ERα silencing promoted ROS
453 production and induced beta cell apoptosis (Zhou et al., 2018). Here, ERα knockdown or

454 treatment with the ERα antagonist MPP induced beta cell apoptosis, reinforcing an
455 antiapoptotic role of this receptor even in the absence of added ligands. In the presence
456 of ER ligands, we observed two different scenarios: while an ERα agonist had no effect
457 on viability, BPA induced ROS production and beta cell apoptosis, indicating that BPA
458 disrupts ERα antiapoptotic role. Our findings indicate that ERβ also plays a pro-survival
459 role in beta cells, as either its silencing or antagonism with PHTPP leads to apoptosis.
460 Interestingly, the percentage of apoptosis in ERβ-silenced cells were much higher than in
461 ERα-deficient cells, suggesting that ERβ might be more important for beta cell survival.
462 BPA effect on apoptosis was abrogated in ERβ-inhibited cells, indicating that, as for ERα,
463 ERβ is also involved in BPA-induced apoptosis. The antiapoptotic protection conferred
464 by ERs is in line with previous findings in islets from ERα and ERβ knockout mice (Liu
465 et al., 2009).
466 After ligand binding, ERα and ERβ form homo- and heterodimers to perform their
467 biological effects (Levin and Hammes, 2016). Different ER ligands stabilize ERα and
468 ERβ homo- and heterodimers in a variety of combinations that mediate the effect of those
469 ER ligands (Paulmurugan et al., 2011). Our bioinformatic results predicted that E2 favors
470 the formation of ERαα, ERββ and ERαβ. BPA, however, stabilized ERββ but did not
471 stabilize ERαβ heterodimers. Based on these results we proposed a model where, in basal
472 conditions, ERαα, ERββ and ERαβ are antiapoptotic. Upon binding, E2 would favor
473 ERαβ heterodimers as well as ERαα and ERββ homodimers, thus protecting beta cells
474 from apoptosis. Conversely, ERαβ heterodimer formation does not occur in the presence
475 of BPA; in fact, the number of ERαβ heterodimers is even decreased by BPA exposure.
476 Therefore, as one of the three ER branches promoting survival is missing, there is an
477 increase in apoptosis (Fig. 8).
478 A direct effect of BPA on ERα and ERβ heterodimerization might explain the part of the
479 BPA apoptotic effect that is neither blocked by GPER antagonism nor fully achieved by
480 GPER activation. Nonetheless, we demonstrated that GPER activation by either BPA or
481 G1 contributes to beta cell apoptosis. As BPA binds to GPER in other cell systems
482 (Thomas and Dong, 2006) and induces rapid nongenomic effects (Chevalier et al., 2014),
483 it is plausible to assume that BPA acts as a GPER agonist in beta cells. As G1 and BPA
484 effects were abolished in the presence of an ER antagonist, after ER knockdown and in
485 islets cells from BERKO mice, we suggest that ERα and ERβ are responsible for the effect
486 of GPER activation. A crosstalk between GPER and ERα has been described for E2 and
487 environmental estrogens (Qie et al., 2021). Remarkably, E2, which also binds to and

488 activates GPER (Revankar et al., 2005; Thomas et al., 2005), does not behave as G1 or
489 BPA. Although these differences remain elusive, our data indicate that they might be
490 related to the E2-induced increase in ERαβ heterodimer formation (Fig. 8).
491 Thus, along with BPA effects on insulin secretion and insulin sensitivity, BPA-induced
492 apoptosis described by us (present data) and others (Carchia et al., 2015; Lin et al., 2013)
493 might contribute to elucidate the diabetogenic effects of BPA described above. In the
494 present work, BPA induces apoptosis at doses within the pico- and nanomolar range,
495 which agrees with both *in vivo* and *in vitro* studies showing that BPA have effects at low
496 doses (Soto et al., 2021; vom Saal and Vandenberg, 2021). Although BPA shows a low
497 affinity for ERα and ERβ (Kuiper et al., 1998; Molina-Molina et al., 2013) and binds to
498 GPER with an IC_{50} of 630 nM (Thomas and Dong, 2006), it is plausible to expect that an
499 amplification of the response to BPA caused by the crosstalk among the three ERs
500 contributes to the proapoptotic effect induced by low concentrations of BPA.
501 Currently, there is a lack of methods for testing EDCs that disrupt metabolism and
502 metabolic functions (Legler et al., 2020). The MIE triggered by BPA and the subsequent
503 increase in ROS production should help to develop novel cellular testing methods to
504 identify other EDCs with diabetogenic properties. Moreover, our results reinforce the
505 need to incorporate ERα and ERβ homodimer and heterodimer formation in the tests to
506 identify EDCs, as it has been already proposed for ERα dimer formation (Kim et al.,
507 2021). Finally, the MIE described herein reflects the complexity of the molecular
508 mechanisms underlying EDC actions. Such complexity complicates the prediction of a
509 given EDC effect without having exact knowledge of the MIE involved. To acquire this
510 knowledge is a long-term goal and, therefore, a deep understanding of the MIEs should
511 not be a strict requirement to create public health policies on EDCs (Soto and
512 Sonnenschein, 2018).
513

514 **5. Conclusions**

515 The three estrogen receptors, ERα, ERβ and GPER, protect beta cells from apoptosis in
516 basal conditions. Low doses of BPA increased beta cell apoptosis in three different cell
517 models, namely dispersed mouse islet cells, the rat beta cell line INS-1E, and the human
518 beta cell line EndoC-βH1. Our data indicate that EndoC-βH1 cells work as a proper
519 human cell model for the identification of EDCs with diabetogenic activity.
520 The pro-apoptotic effect of BPA involves a crosstalk among the three estrogen receptors.
521 Activation of GPER by G1 or BPA induced apoptosis via ERα and ERβ. Our results

522 indicate that BPA directly decreases ERαβ heterodimers via ERα and ERβ or after
523 activation of GPER. This decrease in ERαβ heterodimers disrupts the active antiapoptotic
524 effect of ERα and ERβ in beta cells. Our results should help to develop new test methods
525 to identify diabetogenic EDCs based on the use of human EndoC-βH1 cells, GPER
526 activation, ROS production, and homo- and heterodimerization of ERα and ERβ.
527

528 **Author contributions**

529 LM and AN conceived the study. IB-C, RSDS, RMM-G, AAP-S, J-AE and LM collected
530 and analyzed the data. IB-C, RSDS, RMM-G, AAP-S, J-AE, JM-P, LM and AN
531 interpreted the data. RSDS, JM-P and AN drafted the manuscript. AN and LM supervised
532 the study. RSDS, JM-P, J-AG critically revised the manuscript for important intellectual
533 content. J-AG, J-AE, LM, JM-P and AN acquired the funding. All authors reviewed and
534 approved the final version of the manuscript, and gave consent to publication. LM and
535 AN are responsible for the integrity of the work as a whole.
536

537 **Declaration of Competing Interest**

538 The authors declare that they have no known competing financial interests or personal
539 relationships that could have appeared to influence the work reported in this paper.
540

541 **Acknowledgements**

542 The authors thank Maria Luisa Navarro, Salomé Ramon, and Beatriz Bonmati Botella for
543 their excellent technical assistance. We are grateful to the Cluster of Scientific Computing
544 (http://ccc.umh.es/) of the Universidad Miguel Hernández de Elche for providing
545 computing facilities.
546

547 **Funding**

548 This work was supported by Ministerio de Ciencia e Innovación, Agencia Estatal de
549 Investigación (AEI) and Fondo Europeo de Desarrollo Regional (FEDER) grants
550 BPU2017-86579-R (AN), PID2020-117294RB-I00 (AN, JM-P), Generalitat Valenciana
551 PROMETEO II/2020/006 (AN) and European Union's Horizon 2020 research and
552 innovation programme under grant agreement GOLIATH No. 825489 (AN). Author
553 laboratories hold grants from Ministerio de Ciencia e Innovación, Agencia Estatal de
554 Investigación y Fondo Europeo de Desarrollo Regional (FEDER) RTI2018-096724-B-
555 C21 (J-AE) and PID2020-117569RA-I00 (LM). PROMETEO/2016/006 (J-AE) and

556 SEJI/2018/023 (LM) supported by Generalitat Valenciana, Spain. Robert A. Welch
557 Foundation (grant E-0004) (J-AG). CIBERDEM is an initiative of the Instituto de Salud
558 Carlos III.

559

560 **References**

561 Allen, T.E.H., Goodman, J.M., Gutsell, S., Russell, P.J., 2014. Defining Molecular Initiating Events
562 in the Adverse Outcome Pathway Framework for Risk Assessment. Chemical Research in
563 Toxicology 27, 2100–2112. https://doi.org/10.1021/tx500345j

564 Alonso-Magdalena, P., García-Arévalo, M., Quesada, I., Nadal, Á., 2015. Bisphenol-A treatment
565 during pregnancy in mice: A new window of susceptibility for the development of
566 diabetes in mothers later in life. Endocrinology 156. https://doi.org/10.1210/en.2014-
567 1952

568 Alonso-Magdalena, P., Morimoto, S., Ripoll, C., Fuentes, E., Nadal, A., 2006. The estrogenic
569 effect of bisphenol A disrupts pancreatic beta-cell function in vivo and induces insulin
570 resistance. Environmental Health Perspectives 114, 106–112.
571 https://doi.org/10.1289/ehp.8451

572 Alonso-Magdalena, P., Quesada, I., Nadal, A., 2011. Endocrine disruptors in the etiology of type
573 2 diabetes mellitus. Nature Reviews Endocrinology 7, 346–353.
574 https://doi.org/10.1038/nrendo.2011.56

575 Alonso-Magdalena, P., Ropero, A.B., Carrera, M.P., Cederroth, C.R., Baquie, M., Gauthier, B.R.,
576 Nef, S., Stefani, E., Nadal, A., 2008. Pancreatic insulin content regulation by the estrogen
577 receptor ER alpha. PLoS One 3, e2069. https://doi.org/10.1371/journal.pone.0002069

578 Alonso-Magdalena, P., Vieira, E., Soriano, S., Menes, L., Burks, D., Quesada, I., Nadal, A., 2010.
579 Bisphenol A exposure during pregnancy disrupts glucose homeostasis in mothers and
580 adult male offspring. Environmental Health Perspectives 118, 1243–1250.
581 https://doi.org/10.1289/ehp.1001993

582 Balhuizen, A., Kumar, R., Amisten, S., Lundquist, I., Salehi, A., 2010. Activation of G protein-
583 coupled receptor 30 modulates hormone secretion and counteracts cytokine-induced
584 apoptosis in pancreatic islets of female mice. Molecular and Cellular Endocrinology 320,
585 16–24. https://doi.org/10.1016/j.mce.2010.01.030

586 Bansal, A., Rashid, C., Xin, F., Li, C., Polyak, E., Duemler, A., van der Meer, T., Stefaniak, M.,
587 Wajid, S., Doliba, N., Bartolomei, M.S., Simmons, R.A., 2017. Sex- and dose-specific
588 effects of maternal bisphenol A exposure on pancreatic islets of first- and second-
589 generation adult mice offspring. Environmental Health Perspectives 125.
590 https://doi.org/10.1289/EHP1674

591 Biasini, M., Bienert, S., Waterhouse, A., Arnold, K., Studer, G., Schmidt, T., Kiefer, F., Cassarino,
592 T.G., Bertoni, M., Bordoli, L., Schwede, T., 2014. SWISS-MODEL: Modelling protein
593 tertiary and quaternary structure using evolutionary information. Nucleic Acids Research
594 42. https://doi.org/10.1093/nar/gku340

595 Cabaton, N.J., Canlet, C., Wadia, P.R., Tremblay-Franco, M., Gautier, R., Molina, J.,
596 Sonnenschein, C., Cravedi, J.-P., Rubin, B.S., Soto, A.M., Zalko, D., 2013. Effects of low

597 doses of bisphenol A on the metabolome of perinatally exposed CD-1 mice.
598 Environmental Health Perspectives 121, 586–93. https://doi.org/10.1289/ehp.1205588

599 Carchia, E., Porreca, I., Almeida, P.J., D'Angelo, F., Cuomo, D., Ceccarelli, M., Felice, M. de,
600 Mallardo, M., Ambrosino, C., 2015. Evaluation of low doses BPA-induced perturbation of
601 glycemia by toxicogenomics points to a primary role of pancreatic islets and to the
602 mechanism of toxicity. Cell Death and Disease 6. https://doi.org/10.1038/cddis.2015.319

603 Chevalier, N., Paul-Bellon, R., Camparo, P., Michiels, J.F., Chevallier, D., Fénichel, P., 2014.
604 Genetic variants of GPER/GPR30, a novel estrogen-related G protein receptor, are
605 associated with human seminoma. International Journal of Molecular Sciences 15, 1574–
606 1589. https://doi.org/10.3390/ijms15011574

607 Contreras, J.L., Smyth, C.A., Bilbao, G., Young, C.J., Thompson, J.A., Eckhoff, D.E., 2002. 17β-
608 estradiol protects isolated human pancreatic islets against proinflammatory cytokine-
609 induced cell death: Molecular mechanisms and islet functionality. Transplantation 74.
610 https://doi.org/10.1097/00007890-200211150-00010

611 Cunha, D.A., Cito, M., Carlsson, P.O., Vanderwinden, J.M., Molkentin, J.D., Bugliani, M.,
612 Marchetti, P., Eizirik, D.L., Cnop, M., 2016. Thrombospondin 1 protects pancreatic β-cells
613 from lipotoxicity via the PERK-NRF2 pathway. Cell Death and Differentiation 23.
614 https://doi.org/10.1038/cdd.2016.89

615 Delgado, J., Radusky, L.G., Cianferoni, D., Serrano, L., 2019. FoldX 5.0: Working with RNA, small
616 molecules and a new graphical interface. Bioinformatics 35.
617 https://doi.org/10.1093/bioinformatics/btz184

618 Denizot, F., Lang, R., 1986. Rapid colorimetric assay for cell growth and survival. Modifications
619 to the tetrazolium dye procedure giving improved sensitivity and reliability. Journal of
620 Immunological Methods 89, 271–7. https://doi.org/10.1016/0022-1759(86)90368-6

621 Eizirik, D.L., Pasquali, L., Cnop, M., 2020. Pancreatic beta-cells in type 1 and type 2 diabetes
622 mellitus: different pathways to failure. Nature Reviews Endocrinology 16, 349–362.
623 https://doi.org/10.1038/s41574-020-0355-7

624 Gannon, M., Kulkarni, R.N., Tse, H.M., Mauvais-Jarvis, F., 2018. Sex differences underlying
625 pancreatic islet biology and its dysfunction. Molecular Metabolism 15, 82–91.
626 https://doi.org/10.1016/j.molmet.2018.05.017

627 Gore, A.C., Chappell, V.A., Fenton, S.E., Flaws, J.A., Nadal, A., Prins, G.S., Toppari, J., Zoeller,
628 R.T., 2015. EDC-2: The Endocrine Society's Second Scientific Statement on Endocrine-
629 Disrupting Chemicals. Endocrine Reviews 36. https://doi.org/10.1210/er.2015-1010

630 Heldring, N., Pike, A., Andersson, S., Matthews, J., Cheng, G., Hartman, J., Tujague, M., Strom,
631 A., Treuter, E., Warner, M., Gustafsson, J.A., 2007. Estrogen receptors: how do they signal
632 and what are their targets. Physiological Reviews 87, 905–931.
633 https://doi.org/10.1152/physrev.00026.2006

634 Iwabuchi, E., Miki, Y., Ono, K., Onodera, Y., Suzuki, T., Hirakawa, H., Ishida, T., Ohuchi, N.,
635 Sasano, H., 2017. In situ detection of estrogen receptor dimers in breast carcinoma cells
636 in archival materials using proximity ligation assay (PLA). Journal of Steroids Biochemistry
637 and Molecular Biology 165, 159–169. https://doi.org/10.1016/j.jsbmb.2016.05.022

638 Kang, L., Zhang, X., Xie, Y., Tu, Y., Wang, D., Liu, Z., Wang, Z.Y., 2010. Involvement of estrogen
639 receptor variant ER-alpha36, not GPR30, in nongenomic estrogen signaling. Molecular
640 Endocrinology 24, 709–721. https://doi.org/10.1210/me.2009-0317

641 Kautzky-Willer, A., Harreiter, J., Pacini, G., 2016. Sex and Gender Differences in Risk,
642 Pathophysiology and Complications of Type 2 Diabetes Mellitus. Endocrine Reviews 37,
643 278–316. https://doi.org/10.1210/er.2015-1137

644 Kim, H.M., Seo, H., Park, Y., Lee, H.-S., Lee, S.-H., Ko, K.S., 2021. Development of a Human
645 Estrogen Receptor Dimerization Assay for the Estrogenic Endocrine-Disrupting Chemicals
646 Using Bioluminescence Resonance Energy Transfer. International Journal of
647 Environmental Research and Public Health 18. https://doi.org/10.3390/ijerph18168875

648 Kooptiwut, S., Kaewin, S., Semprasert, N., Sujjitjoon, J., Junking, M., Suksri, K., Yenchitsomanus,
649 P. thai, 2018. Estradiol Prevents High Glucose-Induced β-cell Apoptosis by Decreased
650 BTG2 Expression. Scientific Reports 8. https://doi.org/10.1038/s41598-018-30698-x

651 Krege, J.H., Hodgin, J.B., Couse, J.F., Enmark, E., Warner, M., Mahler, J.F., Sar, M., Korach, K.S.,
652 Gustafsson, J.Å., Smithies, O., 1998. Generation and reproductive phenotypes of mice
653 lacking estrogen receptor β. Proceedings of the National Academy of Sciences of the
654 United States of America 95. https://doi.org/10.1073/pnas.95.26.15677

655 Kuiper, G.G., Carlsson, B., Grandien, K., Enmark, E., Haggblad, J., Nilsson, S., Gustafsson, J.A.,
656 1997. Comparison of the ligand binding specificity and transcript tissue distribution of
657 estrogen receptors alpha and beta. Endocrinology 138, 863–870.
658 https://doi.org/10.1210/endo.138.3.4979

659 Kuiper, G.G., Lemmen, J.G., Carlsson, B., Corton, J.C., Safe, S.H., van der Saag, P.T., van der
660 Burg, B., Gustafsson, J.A., 1998. Interaction of estrogenic chemicals and phytoestrogens
661 with estrogen receptor beta. Endocrinology 139, 4252–63.
662 https://doi.org/10.1210/endo.139.10.6216

663 Legler, J., Zalko, D., Jourdan, F., Jacobs, M., Fromenty, B., Balaguer, P., Bourguet, W., Kos, V.M.,
664 Nadal, A., Beausoleil, C., Cristobal, S., Remy, S., Ermler, S., Margiotta-Casaluci, L., Griffin,
665 J.L., Blumberg, B., Chesné, C., Hoffmann, S., Andersson, P.L., Kamstra, J.H., 2020. The
666 goliath project: Towards an internationally harmonised approach for testing metabolism
667 disrupting compounds. International Journal of Molecular Sciences 21.
668 https://doi.org/10.3390/ijms21103480

669 le May, C., Chu, K., Hu, M., Ortega, C.S., Simpson, E.R., Korach, K.S., Tsai, M.J., Mauvais-Jarvis,
670 F., 2006. Estrogens protect pancreatic beta-cells from apoptosis and prevent insulin-
671 deficient diabetes mellitus in mice. Proceedings of the National Academy of Sciences of
672 the United States of America 103, 9232–9237. https://doi.org/10.1073/pnas.0602956103

673 Levin, E.R., Hammes, S.R., 2016. Nuclear receptors outside the nucleus: extranuclear signalling
674 by steroid receptors. Nature Reviews Molecular Cellular Biology 17, 783–797.
675 https://doi.org/10.1038/nrm.2016.122

676 Lin, Y., Sun, X., Qiu, L., Wei, J., Huang, Q., Fang, C., Ye, T., Kang, M., Shen, H., Dong, S., 2013.
677 Exposure to bisphenol A induces dysfunction of insulin secretion and apoptosis through
678 the damage of mitochondria in rat insulinoma (INS-1) cells. Cell Death and Disease 4,
679 e460. https://doi.org/10.1038/cddis.2012.206

680 Liu, S., le May, C., Wong, W.P., Ward, R.D., Clegg, D.J., Marcelli, M., Korach, K.S., Mauvais-
681 Jarvis, F., 2009. Importance of extranuclear estrogen receptor-alpha and membrane G
682 protein-coupled estrogen receptor in pancreatic islet survival. Diabetes 58, 2292–2302.
683 https://doi.org/10.2337/db09-0257

684 Li, Y., Perera, L., Coons, L.A., Burns, K.A., Tyler Ramsey, J., Pelch, K.E., Houtman, R., van
685 Beuningen, R., Teng, C.T., Korach, K.S., 2018. Differential in vitro biological action,
686 coregulator interactions, and molecular dynamic analysis of bisphenol A (BPA), BPAF, and
687 BPS ligand–ERα complexes. Environmental Health Perspectives 126.
688 https://doi.org/10.1289/EHP2505

689 Marroqui, L., dos Santos, R.S., Fløyel, T., Grieco, F.A., Santin, I., op de Beeck, A., Marselli, L.,
690 Marchetti, P., Pociot, F., Eizirik, D.L., 2015. TYK2, a Candidate Gene for Type 1 Diabetes,
691 Modulates Apoptosis and the Innate Immune Response in Human Pancreatic β-Cells.
692 Diabetes 64, 3808–17. https://doi.org/10.2337/db15-0362

693 Marroqui, L., Martinez-Pinna, J., Castellano-Munoz, M., dos Santos, R.S., Medina-Gali, R.M.,
694 Soriano, S., Quesada, I., Gustafsson, J.A., Encinar, J.A., Nadal, A., 2021. Bisphenol-S and
695 Bisphenol-F alter mouse pancreatic beta-cell ion channel expression and activity and
696 insulin release through an estrogen receptor ERbeta mediated pathway. Chemosphere
697 265, 129051. https://doi.org/10.1016/j.chemosphere.2020.129051

698 Martinez-Pinna, J., Marroqui, L., Hmadcha, A., Lopez-Beas, J., Soriano, S., Villar-Pazos, S.,
699 Alonso-Magdalena, P., dos Santos, R.S., Quesada, I., Martin, F., Soria, B., Gustafsson, J.A.,
700 Nadal, A., 2019. Oestrogen receptor beta mediates the actions of bisphenol-A on ion
701 channel expression in mouse pancreatic beta cells. Diabetologia 62, 1667–1680.
702 https://doi.org/10.1007/s00125-019-4925-y

703 Molina-Molina, J.M., Amaya, E., Grimaldi, M., Sáenz, J.M., Real, M., Fernández, M.F., Balaguer,
704 P., Olea, N., 2013. In vitro study on the agonistic and antagonistic activities of bisphenol-S
705 and other bisphenol-A congeners and derivatives via nuclear receptors. Toxicology and
706 Applied Pharmacology 272. https://doi.org/10.1016/j.taap.2013.05.015

707 Mosmann, T., 1983. Rapid colorimetric assay for cellular growth and survival: application to
708 proliferation and cytotoxicity assays. Journal of Immunological Methods 65, 55–63.
709 https://doi.org/10.1016/0022-1759(83)90303-4

710 Paulmurugan, R., Tamrazi, A., Massoud, T.F., Katzenellenbogen, J.A., Gambhir, S.S., 2011. In
711 vitro and in vivo molecular imaging of estrogen receptor α and β homo-and
712 heterodimerization: Exploration of new modes of receptor regulation. Molecular
713 Endocrinology 25, 2029–2040. https://doi.org/10.1210/me.2011-1145

714 Qie, Y., Qin, W., Zhao, K., Liu, C., Zhao, L., Guo, L.H., 2021. Environmental Estrogens and Their
715 Biological Effects through GPER Mediated Signal Pathways. Environmental Pollution.
716 https://doi.org/10.1016/j.envpol.2021.116826

717 Rancière, Fanny, Botton, J., Slama, R., Lacroix, M.Z., Debrauwer, L., Charles, M.A., Roussel,
718 Ronan, Balkau, Beverley, Magliano, D.J., Balkau, B., Ducimetière, P., Eschwège, E.,
719 Rancière, F., Alhenc-Gelas, F., Girault, A., Fumeron, F., Marre, M., Roussel, R., Bonnet, F.,
720 Bonnefond, A., Cauchi, S., Froguel, P., Alençon, Angers, Blois, Caen, Chateauroux,
721 Chartres, Cholet, le Mans, Orléans, Tours, Cogneau, J., Born, C., Caces, E., Cailleau, M.,
722 Lantieri, O., Moreau, J.G., Rakotozafy, F., Tichet, J., Vol, S., 2019. Exposure to bisphenol a

723 and bisphenol s and incident type 2 diabetes: A case-cohort study in the French cohort
724 D.E.S.I.R. Environmental Health Perspectives 127. https://doi.org/10.1289/EHP5159

725 Ravassard, P., Hazhouz, Y., Pechberty, S., Bricout-Neveu, E., Armanet, M., Czernichow, P.,
726 Scharfmann, R., 2011. A genetically engineered human pancreatic β cell line exhibiting
727 glucose-inducible insulin secretion. Journal of Clinical Investigation 121.
728 https://doi.org/10.1172/JCI58447

729 Razandi, M., Pedram, A., Merchenthaler, I., Greene, G.L., Levin, E.R., 2004. Plasma membrane
730 estrogen receptors exist and functions as dimers. Molecular Endocrinology 18, 2854–
731 2865. https://doi.org/10.1210/me.2004-0115

732 Revankar, C.M., Cimino, D.F., Sklar, L.A., Arterburn, J.B., Prossnitz, E.R., 2005. A
733 transmembrane intracellular estrogen receptor mediates rapid cell signaling. Science 307,
734 1625–1630. https://doi.org/10.1126/science.1106943

735 Santin, I., dos Santos, R.S., Eizirik, D.L., 2016. Pancreatic beta cell survival and signaling
736 pathways: Effects of type 1 diabetes-associated genetic variants, in: Methods in
737 Molecular Biology. https://doi.org/10.1007/7651_2015_291

738 Sargis, R.M., Simmons, R.A., 2019. Environmental neglect: endocrine disruptors as
739 underappreciated but potentially modifiable diabetes risk factors. Diabetologia 62, 1811–
740 1822. https://doi.org/10.1007/s00125-019-4940-z

741 Schmittgen, T.D., Livak, K.J., 2008. Analyzing real-time PCR data by the comparative C(T)
742 method. Nature Protocols 3, 1101–8. https://doi.org/10.1038/nprot.2008.73

743 Soriano, S., Alonso-Magdalena, P., Garcia-Arevalo, M., Novials, A., Muhammed, S.J., Salehi, A.,
744 Gustafsson, J.A., Quesada, I., Nadal, A., 2012. Rapid insulinotropic action of low doses of
745 bisphenol-A on mouse and human islets of Langerhans: role of estrogen receptor beta.
746 PLoS One 7, e31109. https://doi.org/10.1371/journal.pone.0031109

747 Soto, A.M., Schaeberle, C.M., Sonnenschein, C., 2021. From Wingspread to CLARITY: a personal
748 trajectory. Nature reviews. Endocrinology 17, 247–256. https://doi.org/10.1038/s41574-
749 020-00460-3

750 Soto, A.M., Sonnenschein, C., 2018. Endocrine disruptors - putting the mechanistic cart before
751 the phenomenological horse. Nature Reviews Endocrinology 14, 317–318.
752 https://doi.org/10.1038/s41574-018-0003-7

753 Stahlhut, R.W., Myers, J.P., Taylor, J.A., Nadal, A., Dyer, J.A., vom Saal, F.S., 2018. Experimental
754 BPA exposure and glucose-stimulated insulin response in adult men and women. Journal
755 of the Endocrine Society 2. https://doi.org/10.1210/js.2018-00151

756 Thomas, P., Dong, J., 2006. Binding and activation of the seven-transmembrane estrogen
757 receptor GPR30 by environmental estrogens: A potential novel mechanism of endocrine
758 disruption. Journal of Steroid Biochemistry and Molecular Biology 102, 175–179.
759 https://doi.org/10.1016/j.jsbmb.2006.09.017

760 Thomas, P., Pang, Y., Filardo, E.J., Dong, J., 2005. Identity of an estrogen membrane receptor
761 coupled to a G protein in human breast cancer cells. Endocrinology 146, 624–632.
762 https://doi.org/10.1210/en.2004-1064

763 Tovchigrechko, A., Vakser, I.A., 2006. GRAMM-X public web server for protein-protein docking.
764 Nucleic Acids Research 34. https://doi.org/10.1093/nar/gkl206

765 Tsonkova, V.G., Sand, F.W., Wolf, X.A., Grunnet, L.G., Kirstine Ringgaard, A., Ingvorsen, C.,
766 Winkel, L., Kalisz, M., Dalgaard, K., Bruun, C., Fels, J.J., Helgstrand, C., Hastrup, S., Öberg,
767 F.K., Vernet, E., Sandrini, M.P.B., Shaw, A.C., Jessen, C., Grønborg, M., Hald, J.,
768 Willenbrock, H., Madsen, D., Wernersson, R., Hansson, L., Jensen, J.N., Plesner, A.,
769 Alanentalo, T., Petersen, M.B.K., Grapin-Botton, A., Honoré, C., Ahnfelt-Rønne, J.,
770 Hecksher-Sørensen, J., Ravassard, P., Madsen, O.D., Rescan, C., Frogne, T., 2018. The
771 EndoC-βH1 cell line is a valid model of human beta cells and applicable for screenings to
772 identify novel drug target candidates. Molecular Metabolism 8, 144–157.
773 https://doi.org/10.1016/j.molmet.2017.12.007

774 Vandenberg, L.N., Chahoud, I., Heindel, J.J., Padmanabhan, V., Paumgartten, F.J., Schoenfelder,
775 G., 2010. Urinary, circulating, and tissue biomonitoring studies indicate widespread
776 exposure to bisphenol A. Environmental Health Perspectives 118, 1055–1070.
777 https://doi.org/10.1289/ehp.0901716

778 Villar-Pazos, S., Martinez-Pinna, J., Castellano-Muñoz, M., Alonso-Magdalena, P., Marroqui, L.,
779 Quesada, I., Gustafsson, J.-A., Nadal, A., 2017. Molecular mechanisms involved in the
780 non-monotonic effect of bisphenol-a on ca2+ entry in mouse pancreatic β-cells. Scientific
781 Reports 7. https://doi.org/10.1038/s41598-017-11995-3

782 vom Saal, F.S., Vandenberg, L.N., 2021. Update on the Health Effects of Bisphenol A:
783 Overwhelming Evidence of Harm. Endocrinology 162.
784 https://doi.org/10.1210/endocr/bqaa171

785 Wang, B., Li, M., Zhao, Z., Lu, J., Chen, Y., Xu, Y., Xu, M., Wang, W., Wang, T., Bi, Y., Ning, G.,
786 2019. Urinary bisphenol A concentration and glucose homeostasis in non-diabetic adults:
787 a repeated-measures, longitudinal study. Diabetologia 62, 1591–1600.
788 https://doi.org/10.1007/s00125-019-4898-x

789 Wang, C., Nguyen, P.H., Pham, K., Huynh, D., Le, T.B., Wang, H., Ren, P., Luo, R., 2016.
790 Calculating protein-ligand binding affinities with MMPBSA: Method and error analysis.
791 Journal of Computational Chemistry 37, 2436–2446. https://doi.org/10.1002/jcc.24467

792 Zhou, Z., Ribas, V., Rajbhandari, P., Drew, B.G., Moore, T.M., Fluitt, A.H., Reddish, B.R.,
793 Whitney, K.A., Georgia, S., Vergnes, L., Reue, K., Liesa, M., Shirihai, O., van der Bliek, A.M.,
794 Chi, N.W., Mahata, S.K., Tiano, J.P., Hewitt, S.C., Tontonoz, P., Korach, K.S., Mauvais-
795 Jarvis, F., Hevener, A.L., 2018. Estrogen receptor protects pancreatic -cells from apoptosis
796 by preserving mitochondrial function and suppressing endoplasmic reticulum stress.
797 Journal of Biological Chemistry 293, 4735–4751.
798 https://doi.org/10.1074/jbc.M117.805069

799

800
801

802 **Figure legends**

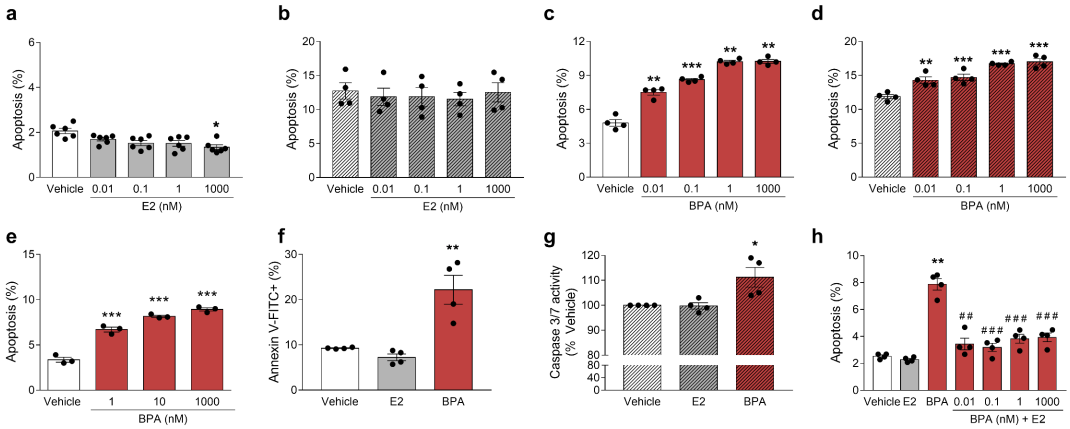

803

804 **Fig. 1 E2 and BPA have different effects on beta cell viability.** INS-1E (**a,c**) and
805 EndoC-βH1 cells (**b,d**) were treated with vehicle (white bars), E2 (grey bars) or BPA (red
806 bars) for 24 h. (**e**) Dispersed islet cells from female mice were treated with vehicle (white
807 bars) or BPA (red bars) for 48 h. Apoptosis was evaluated using Hoechst 33342 and
808 propidium iodide staining. (**f**) INS-1E cells were treated with vehicle (white bar), E2 1
809 nM(grey bar) or BPA 1 nM (red bar) for 48 h. Annexin V-FITC-positive cells were
810 analyzed by flow cytometry. (**g**) EndoC-βH1 cells were treated with vehicle (white bar),
811 E2 1 nM (grey bar) or BPA 1 nM (red bar) for 48 h. Caspase 3/7 activity was measured
812 by a luminescent assay. Results are expressed as % vehicle-treated cells. (**h**) INS-1E were
813 treated with vehicle (white bar), E2 1 nM (grey bar), BPA 1 nM (red bar) or a combination
814 of both (red bars + E2) for 24 h. Apoptosis was evaluated using Hoechst 33342 and
815 propidium iodide staining. Data are shown as means ± SEM of 3-6 independent
816 experiments. (**a-i**) *$p \leq 0.05$, **$p \leq 0.01$ and ***$p \leq 0.001$ vs Vehicle, by one-way ANOVA.
817 (**h**) **$p \leq 0.01$ vs Vehicle; $^{\#\#}p \leq 0.01$ and $^{\#\#\#}p \leq 0.001$ vs BPA 1 nM. One-way ANOVA.

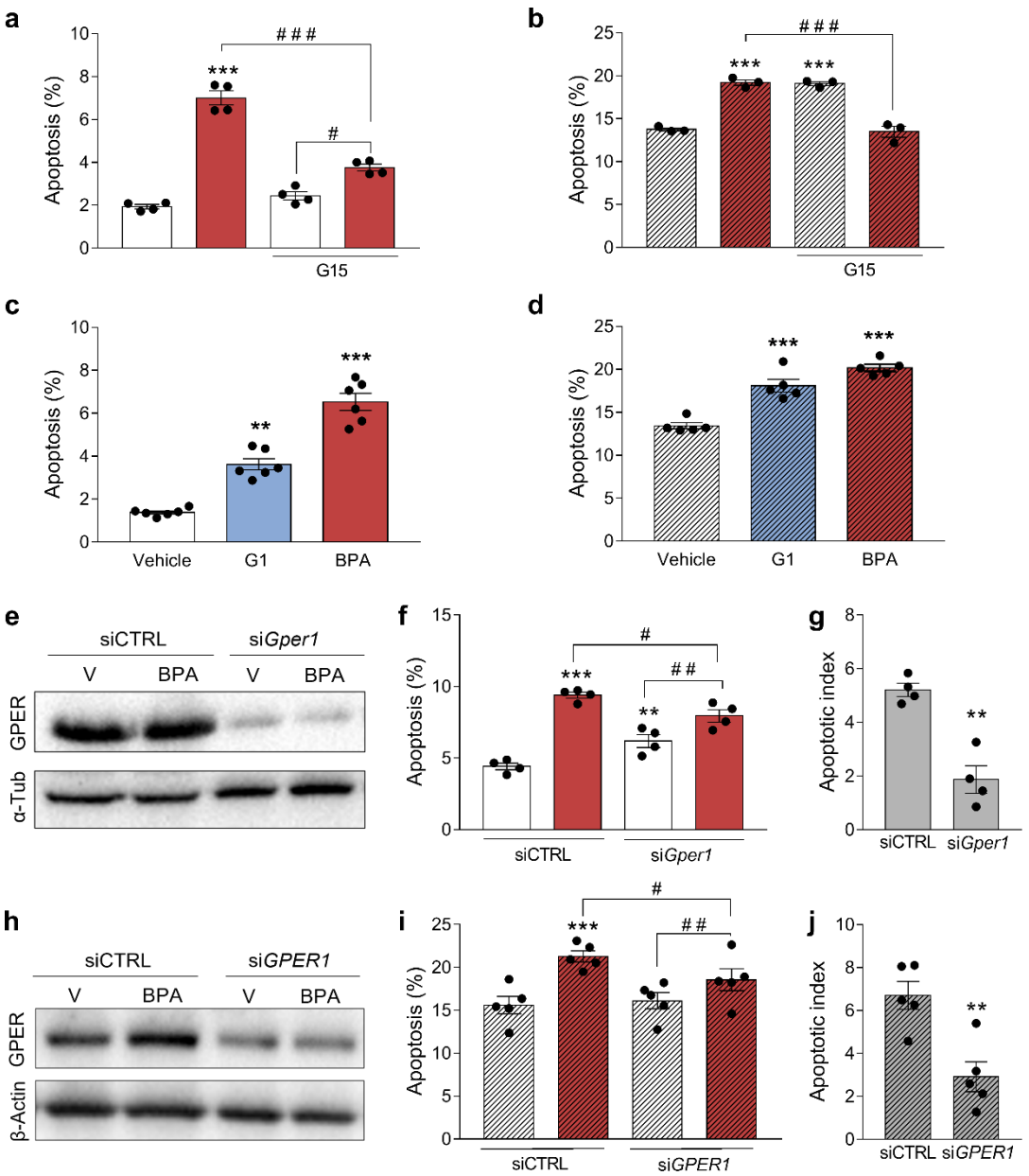

Fig. 2 BPA-induced apoptosis requires GPER. (**a,b**) INS-1E (**a**) and EndoC-βH1 cells (**b**) were pre-treated with vehicle or GPER antagonist G15 10 nM for 3 h. Afterwards, cells were treated with vehicle (white bars) or BPA 1 nM (red bars) in the absence or presence of G15 10 nM for 24 h. (**c,d**) INS-1E (**c**) and EndoC-βH1 cells (**d**) were treated with vehicle (white bars), G1 100 nM (blue bars) or BPA 1 nM (red bars) for 24 h. Apoptosis was evaluated using Hoechst 33342 and propidium iodide staining. (**e-j**) INS-1E (**e-g**) and EndoC-βH1 cells (**h-j**) were transfected with siCTRL or with a siRNA targeting GPER (si*Gper1* or si*GPER1*). Cells were treated with vehicle (white bars) or BPA 1 nM (red bars) for 24 h. (**e,h**) Protein expression was measured by western blot. Representative images of four (**e**) or five (**h**) independent experiments are shown. (**f,i**)

829 Apoptosis was evaluated using Hoechst 33342 and propidium iodide staining. (**g,j**) BPA-
830 induced apoptosis data from Fig. 5f (**g**) and Fig. 5i (**j**) are presented as apoptotic index.
831 Data are shown as means ± SEM of 4-6 independent experiments. (**a,b**) $^{**}p \leq 0.01$ and
832 $^{***}p \leq 0.001$ vs untreated vehicle; $^{\#\#}p \leq 0.01$, $^{\#\#\#}p \leq 0.001$ as indicated by bars. Two-way
833 ANOVA. (**c,d**) $^{**}p \leq 0.01$ and $^{***}p \leq 0.001$ vs vehicle, by one-way ANOVA. (**f,i**)
834 $^{**}p \leq 0.01$ and $^{***}p \leq 0.001$ vs siCTRL vehicle; $^{\#}p \leq 0.05$ and $^{\#\#}p \leq 0.01$ as indicated by bars.
835 Two-way ANOVA. (**g,j**) $^{**}p \leq 0.01$ vs siCTRL, by two-tailed Student's *t* test.
836

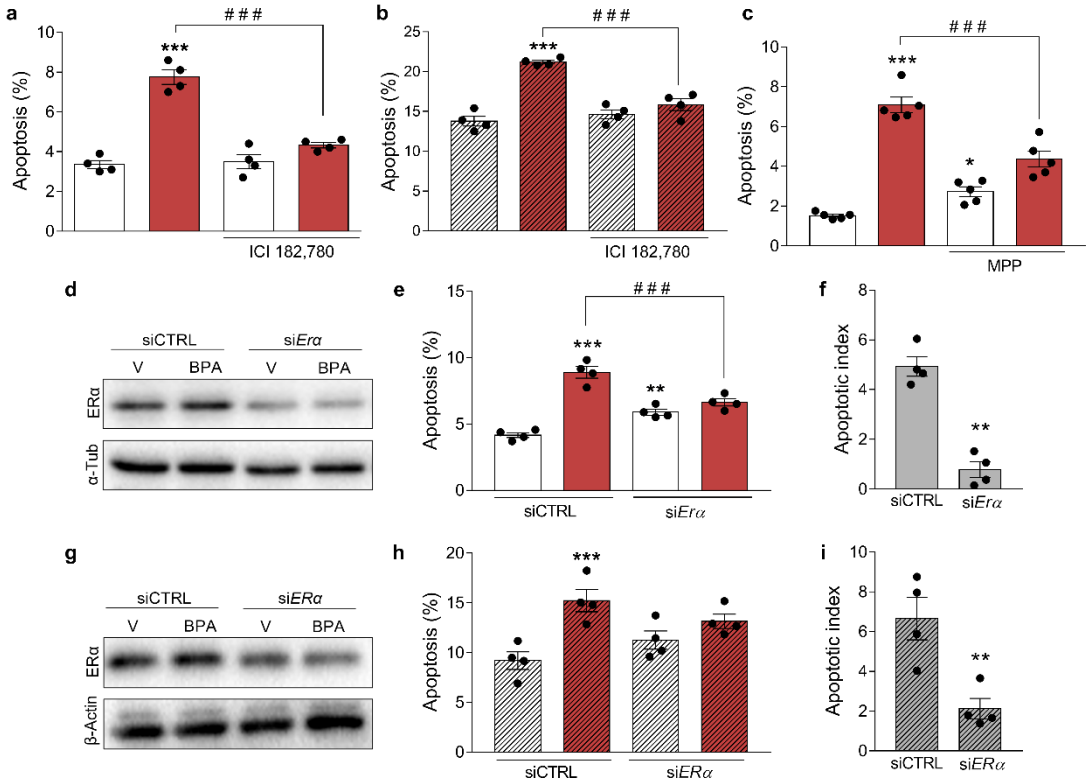

Fig. 3 ERα mediates BPA-induced apoptosis. (**a,b**) INS-1E (**a**) and EndoC-βH1 cells (**b**) were pre-treated with vehicle or antiestrogen ICI 182,780 1 μM for 3 h. Afterwards, cells were treated with vehicle (white bars) or BPA 1 nM (red bars) in the absence or presence of ICI 182,780 1 μM for 24 h. (**c**) INS-1E cells were pre-treated with vehicle or ERα antagonist MPP 100 nM for 3 h. Afterwards, cells were treated with vehicle (white bars) or BPA 1 nM (red bars) in the absence or presence of MPP 100 nM for 24 h. Apoptosis was evaluated using Hoechst 33342 and propidium iodide staining. (**d-i**) INS-1E (**d-f**) and EndoC-βH1 cells (**g-i**) were transfected with siCTRL or with a siRNA targeting ERα (si*Erα* or si*ERα*). Cells were treated with vehicle (white bars) or BPA 1 nM (red bars) for 24 h. (**d,g**) Protein expression was measured by western blot. Representative images of four independent experiments are shown. (**e,h**) Apoptosis was evaluated using Hoechst 33342 and propidium iodide staining. (**g,j**) BPA-induced apoptosis data from Fig. 5e (**f**) and Fig. 5h (**i**) are presented as apoptotic index. Data are shown as means ± SEM of 4-5 independent experiments. (**a-c**) $^{*}p\leq0.05$ and $^{***}p\leq0.001$ vs untreated vehicle; $^{###}p\leq0.001$ as indicated by bars. Two-way ANOVA. (**e,h**) $^{**}p\leq0.01$ and $^{***}p\leq0.001$ vs siCTRL vehicle; $^{###}p\leq0.001$ as indicated by bars. Two-way ANOVA. (**f,i**) $^{**}p\leq0.01$ vs siCTRL, by two-tailed Student's *t* test.

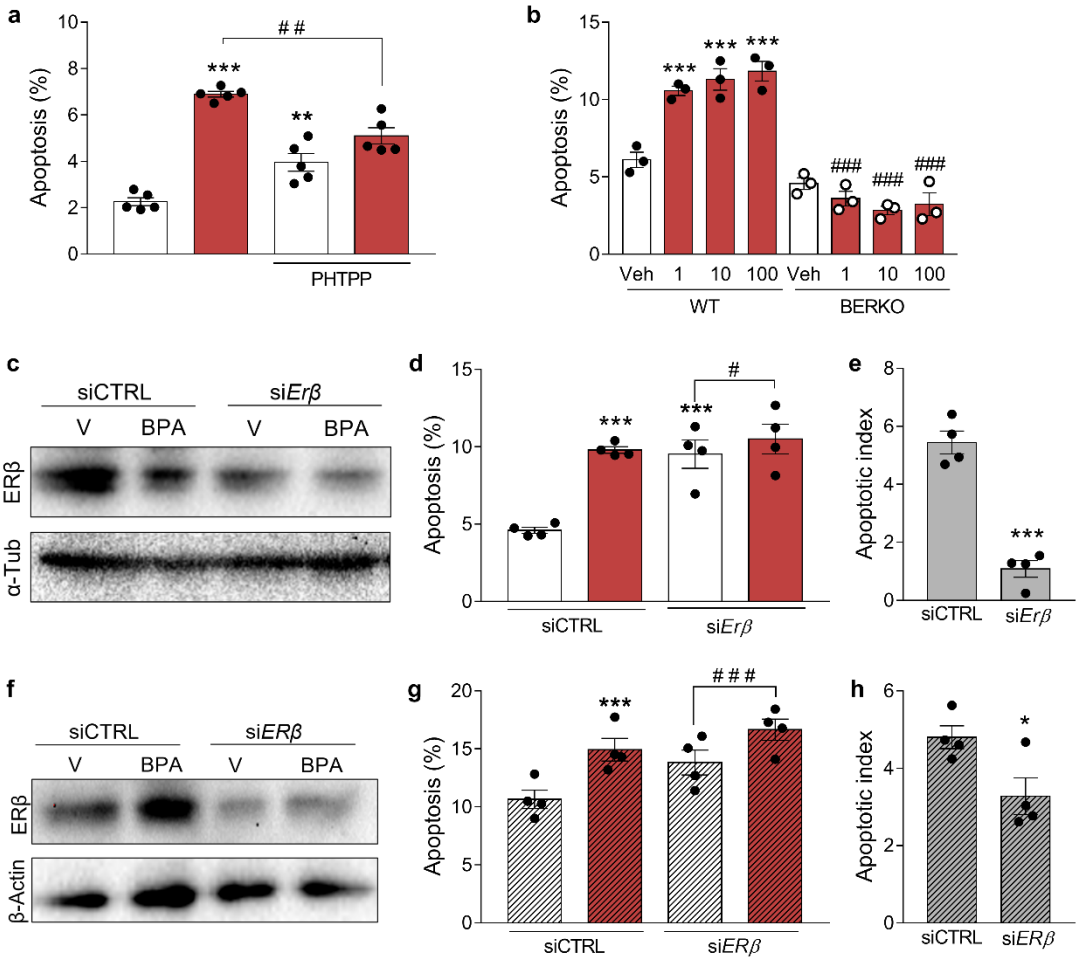

Fig. 4 ERβ mediates BPA-induced apoptosis. (**a**) INS-1E cells were pre-treated with vehicle or ERβ antagonist PHTPP 1 μM for 3 h. Afterwards, cells were treated with vehicle (white bars) or BPA 1 nM (red bars) in the absence or presence of PHTPP 1 μM for 24 h. (**b**) Dispersed islet cells from WT and BERKO mice were treated with vehicle (white bars) or BPA (red bars) for 48 h. Apoptosis was evaluated using Hoechst 33342 and propidium iodide staining. (**c-h**) INS-1E (**c-e**) and EndoC-βH1 cells (**f-h**) were transfected with siCTRL or with a siRNA targeting ERβ (si*Erβ* or si*ERβ*). Cells were treated with vehicle (white bars) or BPA 1 nM (red bars) for 24 h. (**c,f**) Protein expression was measured by western blot. Representative images of four independent experiments are shown. (**d,g**) Apoptosis was evaluated using Hoechst 33342 and propidium iodide staining. (**e,h**) BPA-induced apoptosis data from Fig. 5d (**e**) and Fig. 5g (**h**) are presented as apoptotic index. Data are shown as means ± SEM of 3-5 independent experiments. (**a**) $^{**}p\leq0.01$ and $^{***}p\leq0.001$ vs untreated vehicle; $^{\#\#}p\leq0.01$ as indicated by bars. Two-way ANOVA. (**b**) $^{***}p\leq0.001$ vs WT vehicle; $^{\#\#\#}p\leq0.001$ vs respective WT. Two-way ANOVA. (**d,g**) $^{***}p\leq0.001$ vs siCTRL vehicle; $^{\#}p\leq0.05$ and $^{\#\#\#}p\leq0.001$ as indicated by

872 bars. Two-way ANOVA. (**e,h**) *$p \leq 0.05$ and ***$p \leq 0.001$ vs siCTRL, by two-tailed
873 Student's *t* test.
874

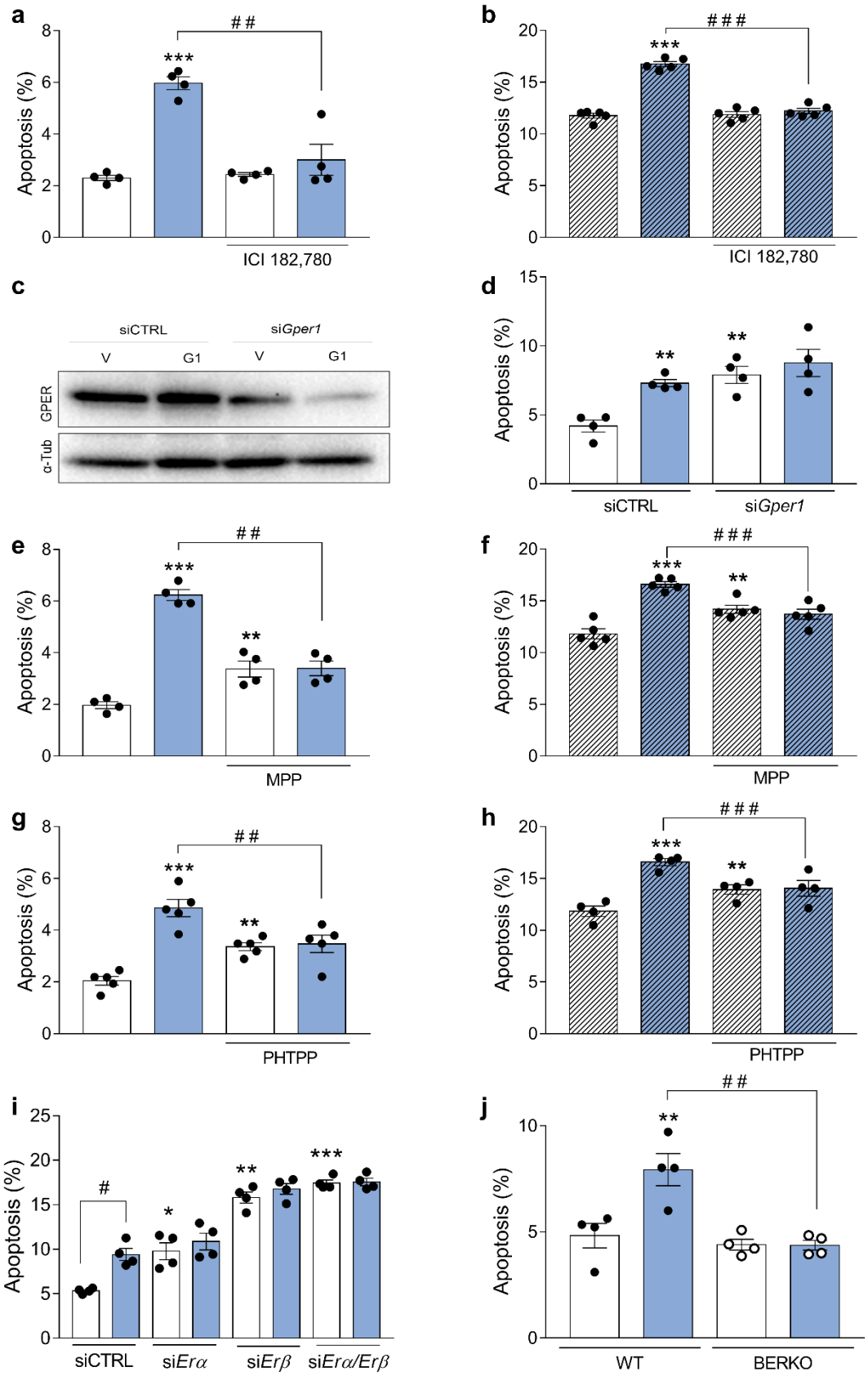

875

876 **Fig. 5 A GPER crosstalk with ERα and ERβ induces apoptosis.** (**a**,**b**) INS-1E (**a**) and

877 EndoC-βH1 cells (**b**) were pre-treated with vehicle or antiestrogen ICI 182,780 1 μM for

878 3 h. Afterwards, cells were treated with vehicle (white bars) or G1 100 nM (blue bars) in
879 the absence or presence of ICI 182,780 1 μM for 24 h. Apoptosis was evaluated using
880 Hoechst 33342 and propidium iodide staining. (**c,d**) INS-1E were transfected with
881 siCTRL or with a siRNA targeting GPER (si*Gper1*). Cells were treated with vehicle
882 (white bars) or G1 100 nM (blue bars) for 24 h. (**c**) Protein expression was measured by
883 western blot. Representative images of four independent experiments are shown. (**d**)
884 Apoptosis was evaluated using Hoechst 33342 and propidium iodide staining. (**e-h**) INS-
885 1E (**e,g**) and EndoC-βH1 cells (**f,h**) were pre-treated with vehicle, ERα antagonist MPP
886 100 nM (**e,f**) or ERβ antagonist PHTPP 1 μM (**g,h**) for 3 h. Afterwards, cells were treated
887 with vehicle (white bars) or G1 100 nM (blue bars) in the absence or presence of MPP
888 100 nM (**e,f**) or PHTPP 1 μM (**g,h**) for 24 h. Apoptosis was evaluated using Hoechst
889 33342 and propidium iodide staining. (**g,h**) INS-1E cells were transfected with siCTRL
890 or siRNAs targeting ERα (si*Erα*) and ERβ (si*Erβ*) or ERα and ERβ simultaneously
891 (si*Erα*/*Erβ*.) Cells were treated with vehicle (white bars) or G1 100 nM (blue bars) for 24
892 h. Apoptosis was evaluated using Hoechst 33342 and propidium iodide staining. (**e**)
893 Dispersed islet cells from WT and BERKO mice were treated with vehicle (white bars)
894 or G1 100 nM (blue bars) for 48 h. Apoptosis was evaluated using Hoechst 33342 and
895 propidium iodide staining. Data are shown as means ± SEM of 4-5 independent
896 experiments. (**a,b,e-h**) $^{**}p\leq0.01$ and $^{***}p\leq0.001$ vs untreated vehicle; $^{\#\#\#}p\leq0.001$ as
897 indicated by bars. Two-way ANOVA. (**d,i**) $^{*}p\leq0.05$, $^{**}p\leq0.01$ and $^{***}p\leq0.001$ vs
898 siCTRL vehicle; $^{\#}p\leq0.001$ as indicated by bars. Two-way ANOVA. (**j**) $^{**}p\leq0.01$ vs WT
899 vehicle; $^{\#\#}p\leq0.01$ as indicated by bars. Two-way ANOVA.
900

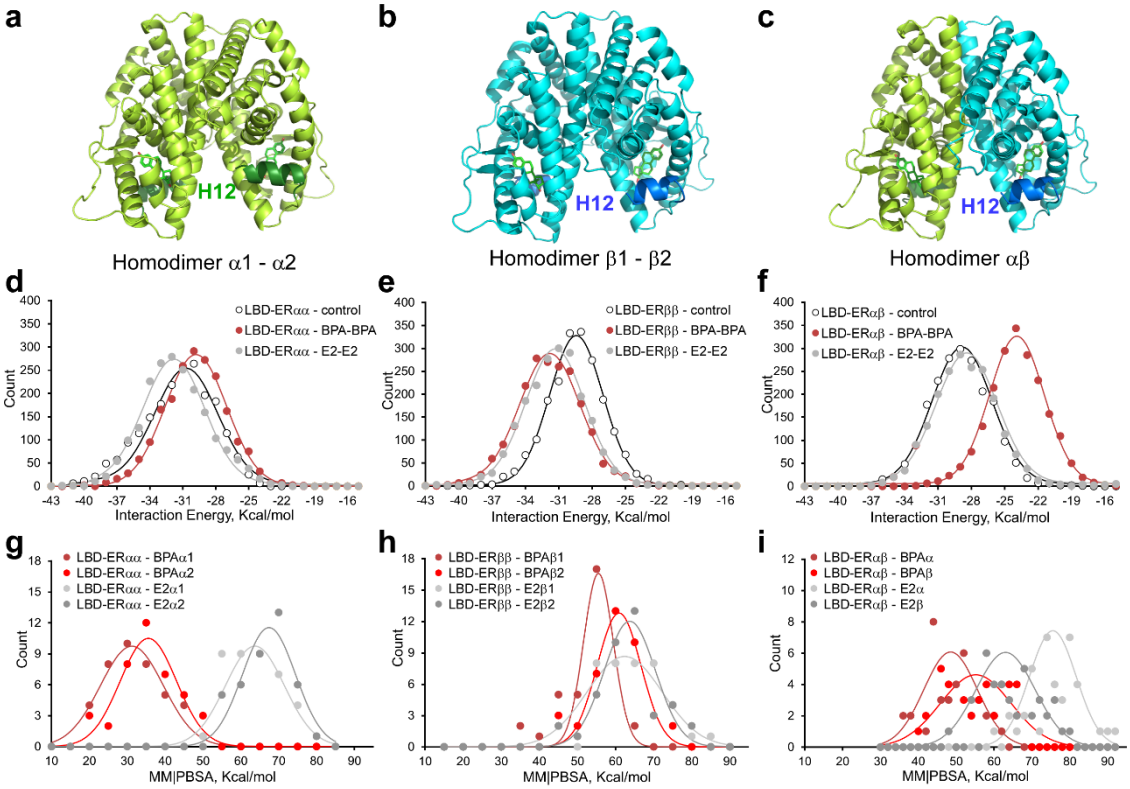

Fig. 6 Effect of BPA and E2 on the molecular dynamics for the LBD of the homodimer- or heterodimer-ER. Secondary structure models of closed LBD-ER as (**a**) alpha homodimer, (**b**) beta homodimer and (**c**) alpha-beta heterodimer. The H12 helix has been colored dark green (alpha monomers) or dark blue (beta monomers). The structure of E2 (green sticks for carbons) is included within the LBD cavities of both subunits. (**d**) Frequency distributions of the intermolecular protein Foldx-calculated interaction energy for the subunits of the alpha homodimer, (**e**) beta homodimer and (**f**) alfa-beta heterodimer in the presence of BPA or E2 ligands in each H12 closed LBD cavity. (**g**) Frequency distributions of the molecular mechanics Poisson–Boltzmann surface area (MM/PBSA) solvation binding energy values of each ligand bound to cavity of the alpha homodimer, (**h**) beta homodimer or (**i**) alpha-beta heterodimer in the presence of BPA or E2 ligands inside of the closed LBD. YASARA software-calculated MM|PBSA values more positive energies indicate better binding of the compound bound to the protein. A Gaussian curve overlaps discrete data.

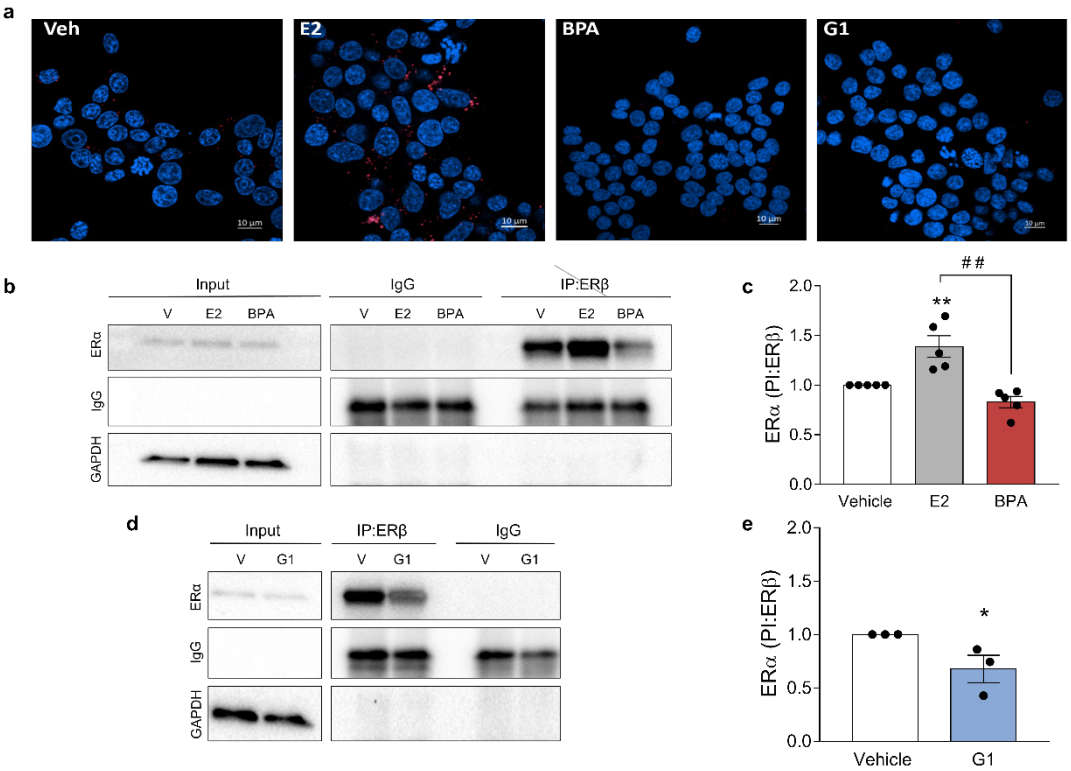

Fig. 7 E2 and BPA have differential effects on ERα/β heterodimer formation. (a) INS-1E cells were treated with vehicle, E2 1 nM, BPA 1 nM or G1 100 nM for 24 h. Heterodimers were detected using in situ proximity ligand assay, where heterodimers are represented as red dots (Texas red) and nuclei are shown in blue (DAPI). (**b-e**) INS-1 E cells were treated with vehicle (white bars), E2 1 nM (grey bars), BPA 1 nM (red bars) (**b,c**) or G1 100 nM (blue bars) (**d,e**) for 24 h. Cells were lysed and proteins collected for co-immunoprecipitation with anti-ERβ antibody. Nonspecific rabbit IgG was used as a negative control. Immunoprecipitates and total protein (Input) expression were measured by western blot. Representative images of three to five independent experiments are shown (**b,d**) and densitometry results are presented for ERα-specific binding to ERβ (**c,e**). Values were normalised by GAPDH and then by the value of vehicle-treated cells of each experiment (considered as 1). Data are shown as means ± SEM of 3-5 independent experiments. (**c**) $^{**}p \leq 0.01$ vs vehicle; $^{\#\#}p \leq 0.01$ as indicated by bars. One-way ANOVA. (**e**) $^{*}p \leq 0.05$ vs vehicle, by two-tailed Student's *t* test.

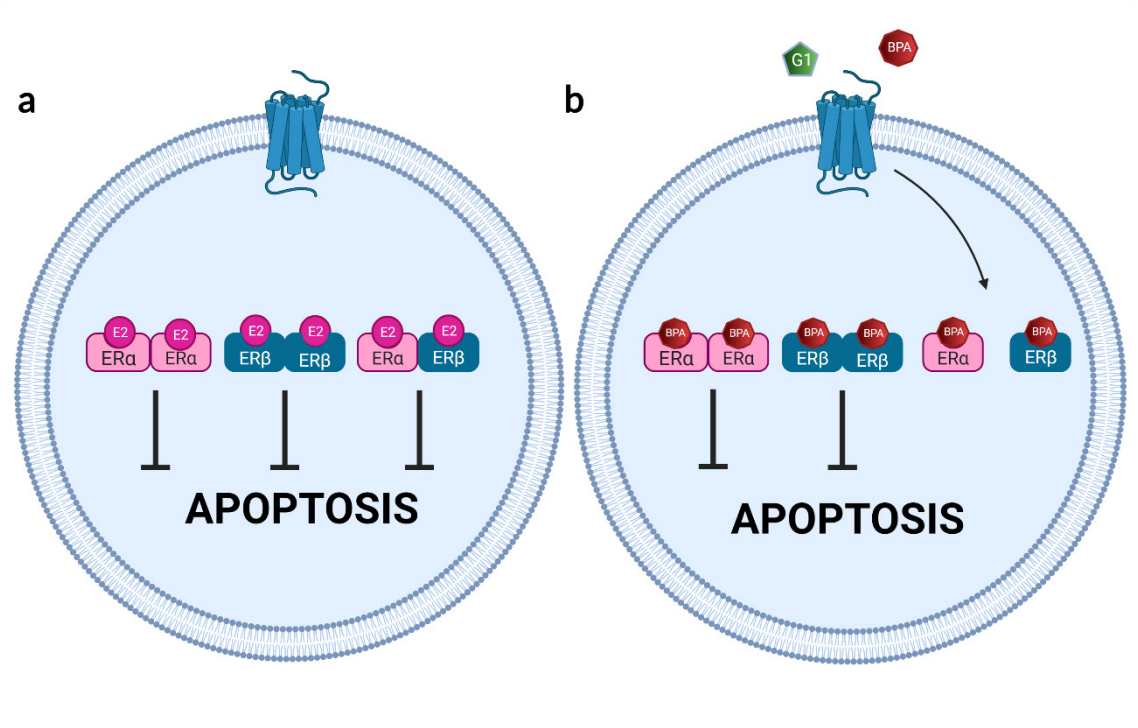

Fig. 8 Scheme summarizing our model for E2 and BPA effects on beta cell apoptosis. (**a**) In basal conditions, ERα, ERβ homodimers and ERαβ heterodimers exist and protect beta cells from apoptosis. These dimers are also stabilized by E2. (**b**) Activation of GPER by G1 or BPA decreases ERαβ heterodimers and increases apoptosis. Binding of BPA to ERα and/or ERβ disfavors ERαβ formation. Created with BioRender.com.